2010

Neutron dosimeter development based on Medipix2

Mohd Amir R. Othman
University of Wollongong, marbo894@uow.edu.au

Marco Petasecca
University of Wollongong, marcop@uow.edu.au

Susanna Guatelli
University of Wollongong, susanna@uow.edu.au

J. Uher
CSIRO Process Science and Engineering

Damion Marinaro
Defence Science and Technology Organisation

See next page for additional authors

Neutron Dosimeter Development Based on Medipix2

Mohd A. R. Othman, M. Petasecca, *Member, IEEE*, S. Guatelli, J. Uher, Damian G. Marinaro, Dale A. Prokopovich, *Member, IEEE*, Mark I. Reinhard, *Member, IEEE*, Michael L. F. Lerch, *Member, IEEE*, J. Jakubek, *Member, IEEE*, S. Pospisil, *Member, IEEE*, and Anatoly B. Rosenfeld, *Senior Member, IEEE*

***Abstract*—A novel neutron dosimetry system for avionics and space applications is described. The new dosimetric system is based on Medipix2, a high density silicon based pixilated detector with integrated readout and digital interface circuitry. Real time dose equivalent response to fast neutron fields with flattened energy response is achieved through the coupling of a structured variable thickness polyethylene (PE) over layer with the high density pixilated detector. Experimental results obtained to 14 MeV D-T and Am-Be neutron fields are described along with a comparison to results obtained with GEANT4 simulations.**

***Index Terms*—GEANT4, Medipix2, neutron dosimetry.**

I. Introduction

EXPOSURE to ionizing radiation in space environments can increase the risk of morbidity and mortality. In addition, radiation damage to electronic components could compromise space mission success and put the wellbeing of the crew at risk. Improving the means to detect and quantify both risk and damage attributable to radiation is an important need.

The radiation environment of space is enhanced relative to that on Earth where the Earth's geomagnetic field and atmosphere provide protection from extra-terrestrial radiation sources. Space radiation is composed of a mix of high energy electrons, protons, and both light and heavy ions [1]. The particles originate from several sources including trapped radiation, galactic cosmic rays (GCR) and solar particle events (SPE). To some extent shielding can be employed to reduce the exposure of astronauts to the primary radiation field. Sufficient shielding to passively attenuate primary radiation to an acceptable level for humans is generally unacceptable from the point of view of spacecraft mass launch limitations. Multilayered shielding can be utilised to reduce the radiobiological effectiveness (RBE) and dose equivalent associated with the secondary radiation field, as well as to address spacecraft weight restrictions. However inadequate shielding design can result in the production of a secondary radiation field which can present greater risk than the primary radiation field on account of enhanced RBE. In an interplanetary mission a female astronaut at age 30 is projected to receive the prescribed limiting dose equivalent equating to a probability of 3% excess fatal cancer at 95% confidence in 54 days. The equivalent duration for a male to reach the same limit is 91 days [2], [3].

Until the early 1990s high-energy heavy ions, such as iron, were considered to be the major radiological hazard. However, Dicello and others [4] noted that secondary neutrons and charged particles of up to several hundred MeV are produced in abundance by the GCR and SPE, as well as the less abundant high energy heavy ions referred as high $-$Z, $-$E (HZE), as these primary radiations pass through the spacecraft or the astronauts. It was further noted that secondary neutrons, produced from the highly abundant primary protons, could be one of the most biologically damaging radiations encountered in space, perhaps comparable in effect to that of the primary HZEs. There has been a lot of ongoing work towards evaluating the relative consequences of HZEs and secondary neutrons at the NASA Space Radiation Lab (NSRL) at Brookhaven National Laboratory and the Loma Linda Proton Therapy Facility during the past decade. These facilities offer heavy ions from 0.1 to 1 GeV/a.m.u. allowing radiobiological effects of space to be studied. An overview of space related radiobiological results obtained at these dedicated radiation beams are well reviewed in [5].

The importance of personnel dosimetry for astronauts is increasing with planned Lunar and Mars missions where the radiation background is less well known in comparison with low earth orbits (LEO). Given the significance of both neutrons and HZEs in determining the dose equivalent it is important that new methods and instrumentation be developed for determining the dose equivalent in real time. Uncertainties in the RBE of such radiations also need further attention.

One of the existing methods widely adapted for real time dose equivalent measurements in space environments is based on microdosimetry. Microdosimetric spectra convoluted with quality coefficients can provide the RBE of radiation and consequently the dose equivalent [6].

During the last decade efforts have been made to develop a solid state microdosimeter to replace bulky high voltage operated tissue equivalent proportional gas counters (TEPC). The detector is based on silicon-on-insulator (SOI) material with an array of sensitive volumes (SV) of individual size similar to that

Manuscript received July 16, 2010; revised September 06, 2010; accepted September 06, 2010. Date of publication October 07, 2010; date of current version December 15, 2010. This work was supported in part by funding from the Commonwealth Government of Australia.

M. A. R. Othman, M. Petasecca, S. Guatelli, M. L. F. Lerch and A. B. Rosenfeld are with the Centre for Medical Radiations Physics, University of Wollongong, NSW 2522, Australia (e-mail: anatoly@uow.edu.au).

J. Uher is with CSIRO Process Science and Engineering, Lucas Heights, NSW 2234, Australia.

D. A. Prokopovich and M. I. Reinhard are with the Australia Nuclear and Technology Organisation (ANSTO), NSW 2234, Australia and also with the Centre for Medical Radiations Physics, University of Wollongong, NSW 2522, Australia.

D. G. Marinaro is with the Defence Science and Technology Organisation, Fishermans Bend, VIC 3207, Australia.

J. Jakubek and S. Pospisil are with the Institute of Experimental and Applied Physics, Czech Technical University in Prague, 12800 Prague 2, Czech Republic.

Color versions of one or more of the figures in this paper are available online at http://ieeexplore.ieee.org.

Digital Object Identifier 10.1109/TNS.2010.2076837

of biological cells [7]–[12]. The principal advantage of the microdosimetric approach is its applicability to any mixed radiation field including those containing charged particles, neutrons and photons.

We have previously demonstrated good agreement of a SOI microdosimeter with TEPC in a standard neutron radiation field facility at CERN typical of high altitude avionic environments (20 to 25 km above sea level) [13]. This field is dominated by secondary neutrons, produced by interactions of GCRs with the atmosphere [14].

In this work we describe a new approach to dose equivalent neutron dosimetry suitable for mixed radiation field applications in avionics and space.

The novel detector has been realized by coupling an *ad-hoc* PE converter to pixilated detector. This detector was primarily developed for X-ray imaging [15], with more recent adoption to neutron imaging through use of suitable converters [16].

The novel detector measures the neutron dose equivalent by counting proton recoil events within the detector pixels which originate from neutron interactions within a variable thickness PE. The ratio of the detector response to the neutron tissue-equivalent dose is almost independent of the energy of the incident neutrons.

In a previous study [17] we demonstrated the possibility of optimizing the thicknesses of the PE segments by means of a GEANT4 simulation in order to obtain an energy-independent detector response proportional to neutron dose equivalent. This paper describes a complementary study consisting of the validation of the GEANT4 simulation with respect to experimental measurements.

II. Design of the Novel Dosimeter

The detection of fast neutrons using silicon radiation detectors and hydrogenous PE converters is well known based on the detection of the recoil protons resulting from the elastic scattering of neutrons with energy E_n on a stationary proton where the recoil proton is scattered under an angle θ with energy E_p given by, $E_p = E_n \cos^2\theta$.

However the response of the silicon detector covered with a uniform hydrogenous converter has several shortcomings:

- — First, it is a tradeoff between thickness of the converter (efficiency of the dosimeter) and the energy range of the detectable fast neutrons.
- — Second, it is not possible to achieve an energy independent response in terms of dose equivalent.
- — Third, the deposition of energy from Compton electrons (gamma radiation) and charged particles present within a mixed radiation field, as well as charged particles from $Si(n,x)$ reactions, produce background events which are undistinguishable from recoil proton events.

Attempts have been made to achieve an improvement in energy response of a single silicon detector by coupling a dual layered PE converter of 0.01 and 1 mm thicknesses in a ratio by area of 17:1 [18]. This led to a variation in the dosimeter response counts/Sv of approximately a factor of two within a neutron energy range of 1–15 MeV. Another approach for fast neutron dosimetry was based on a monolithic $\Delta E - E$ detector by Shiraishi [19] coupled with a PE converter. This system allows measurement of the proton energy E_p and angle of scattered proton θ followed by a determination of the neutron energy and dose equivalent using fluence to dose equivalent conversion factors [20]. This system is limited to relatively low neutron energies on account of the need to stop the recoiling proton within the E detector layer to obtain a full energy measurement. For example, for 0.5 mm silicon the sensitivity is limited to protons of energy less than 8 MeV.

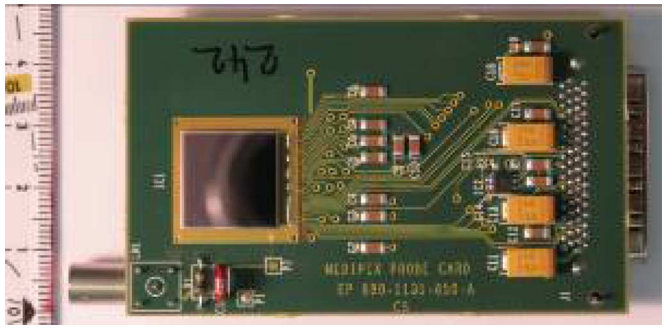

Fig. 1. The Medipix2 board; the sensor can be read out through a USB interface by the software Pixelman.

Our approach is based on a pixilated silicon detector and a structured PE converter that allows independent readout of counts under each partial PE converter. Additionally, the uncovered active area of the pixilated detector is used for subtraction of the background events associated with gamma radiation, charged particles from the space radiation environment and products of direct neutron inelastic reactions within the silicon detector material. By optimizing the thicknesses and total area of particular PE segments it is possible to achieve an energy independent neutron dose equivalent response due to the high level of parameterization that is normally impossible with a single bulk silicon detector. With pixilated detectors it is possible to use an additional degree of adjustment by readout of only part of the area under a partial converter which is controllable by software.

The pixilated detector used in this study was the Medipix2 detector developed originally at CERN ([21] and references therein). Recently Medipix2 has been used for high resolution imaging [16] as well as for thermal and fast neutron fluence monitoring in the high energy physics (HEP) detector barrel as a Radiation Damage Monitoring (RDM) system by use of a partial cover of Medipix2 with ^{6}Li and PE converters [22].

The sensor is composed of a 300 μm thick high resistivity silicon substrate organized as a bi-dimensional array of pad diodes with a pitch of 55 μm and a total sensitive area of 14×14 mm^2 (Fig. 1). The array of diodes has been bump-bonded to a 0.25 μm CMOS ASIC with 65536 charge sensitive amplifiers (CSA), digital-to-analog converter (DAC), two discriminator thresholds, pixel configuration register (PCR), shift register and counter (SR/C) and double discriminator logic [23]. Each pixel is independently readout using Pixelman data acquisition software through an USB interface [24].

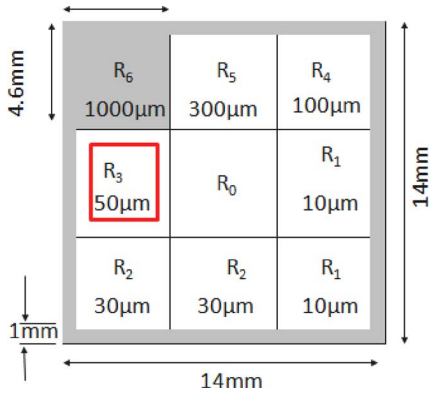

Fig. 2. A simplified arrangement of 3 × 3 segments of different thicknesses of PE converter on the Medipix2 14 × 14 mm^2 active surface area.

III. GEANT4 Simulation and Validation

A. The Simulation Application and Simulated Response

GEANT4 (GEometry ANd Tracking) [25], [26], was adopted as Monte Carlo Simulation Toolkit in this research. GEANT4 describes the interactions of particles with matter, providing advanced functionality in physics and geometry modeling. GEANT4 version 9.2.p01 was used. GEANT4 is a collection of C++ class libraries for radiation transport simulations.

The GEANT4 QGSP_BIC_HP physics list was adopted in this work to describe the electromagnetic and hadronic interactions of the particles involved in the experimental set-up. In particular this physics list uses evaluated cross section databases for neutrons, with energy lower than 20 MeV.

Medipix2 was modelled in GEANT4 with a silicon substrate thickness of 300 μm and a 14 × 14 mm^2 area. 256 × 256 sensitive volume cells were defined across the surface area corresponding with the physical pixels of the Medipix2 system. A dead layer of several microns on the surface of the silicon detector was not modelled in the simulation.

The partial PE converters were selected based on a preliminary analysis which lead to the selection of six different thicknesses of 0.01, 0.03, 0.05, 0.1, 0.3 and 1 mm labelled as R_1, R_2, R_3, R_4, R_5 and R_6 respectively. The layout is presented in Fig. 2. Region R_0 was the uncovered area used to subtract background events associated with gamma-rays, charged particles and products of inelastic neutron interactions with silicon nuclei. The Medipix2 silicon sensitive scoring volume was defined in GEANT4 simulations immediately under each partial PE converter. The red boxes show the possibility of scaling the readout area of each segment to reduce cross talk between segments. This is an additional degree of parameterization allowing adjustment of the energy response of the dosimeter.

Parallel beam primary mono-energetic neutrons with energies from 0.3 to 15 MeV at normal incidence to the detector surface were simulated using the GEANT4 code. Energy deposition events occurring with energies greater than 10 keV in the segments, which is a low energy threshold of the Medipix2 detector, were counted as a single event.

Optimization of the structured converter was performed by taking into account the total response, $R_{\Phi,\mathrm{total}}$, from all partial PE converters such that the $R_{\Phi,\mathrm{total}}$ response is proportional with the ICRP 74 fluence to ambient dose equivalent conversion coefficients, H^*/Φ. This infers that the total number of counts produced by recoil protons per unit dose equivalent in Medipix2 is independent of the neutron energy in the range 0.3–15 MeV. The optimization function for $R_{\Phi,\mathrm{total}}$ is defined by (1)

$$R_{\Phi,\mathrm{total}} = \sum_{i=1}^{9} \beta_{\Phi,i} R_{\Phi,i}(E) \tag{1}$$

$R_{\Phi,1}$ to $R_{\Phi,6}$ are the proton count responses from pixels covered by partial PE of different thickness (Fig. 2) and $R_{\Phi,7}$ to $R_{\Phi,9}$ are the virtual responses given by (2)

$$\begin{aligned} R_{\Phi,7} &= \left(\frac{R_{\Phi,5}}{R_{\Phi,4}}\right) R_{\Phi,1} \\ R_{\Phi,8} &= \left(\frac{R_{\Phi,4}}{R_{\Phi,3}}\right) R_{\Phi,2} \\ R_{\Phi,9} &= \left(\frac{R_{\Phi,2}}{R_{\Phi,3}}\right) R_{\Phi,6} \end{aligned} \tag{2}$$

$\beta_{\Phi,i}$ are the weighting factors for each partial response. The recoil proton counts can be expressed as in (3).

$$R_{\Phi,i} = (R'_{\Phi,i} - (A_i/A_0) R_{\Phi,0})/\Phi_n \tag{3}$$

$R_{\Phi,i}$ and $R'_{\Phi,i}$ are the proton counts and total event counts respectively per neutron fluence under a partial PE segment with thickness i. $R_{\Phi,0}$ is the readout counts from the uncovered segment, A_i is the area of the segment with thickness i and A_0 is the area of the uncovered segment area. Φ_n is the primary neutron fluence.

Virtual responses $R_{\Phi,7}$ to $R_{\Phi,9}$ were introduced for fine tuning of the low energy response ($<$ 1 MeV) and can be neglected in most practical situations, leaving six terms in (1). The energy response of a neutron dosimeter based on Medipix2 with a structured PE converter optimized and modelled with GEANT4 is presented in Fig. 3. The flatness of the neutron energy response was $\pm 9\%$ in the energy range 0.3–15 MeV. This is a substantially better flatness than that achievable with known neutron dosimeters based on a single silicon detector and PE converter.

B. Validation of the GEANT4 Simulation Application and Radiation Setup

In order to quantify the accuracy of the results deriving from the GEANT4 simulation study adopted to optimize the design of the PE layer structure, we validated the GEANT4 application with respect to experimental measurements.

For testing purposes we modeled in the simulation the response of a simplified detector set up with a uniform PE converter to neutrons, exposed to a D-T generator and an Am-Be source.

Fig. 4 shows the experimental set-up of the Medipix2 detector. A significant issue for a neutron dosimeter is the evaluation of the neutron events while separating the background radiation generated, for example, by alphas, gammas and electrons. The use of a large area and high density pixilated detector such as the Medipix2 (with cross section equal to 14 × 14 mm^2 and

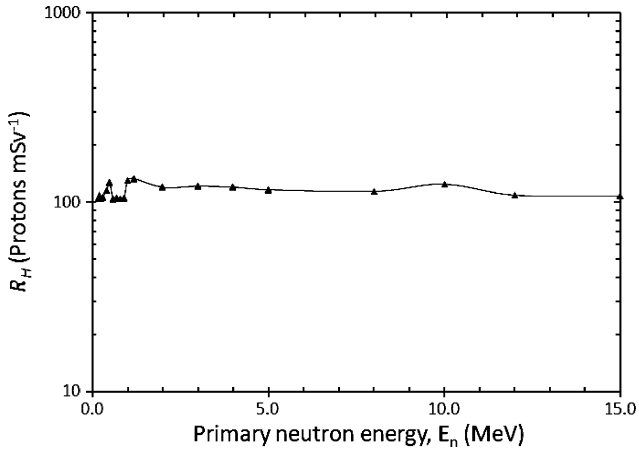

Fig. 3. Dose equivalent energy response of simulated neutron dosimeter with structured PE converter according to (1).

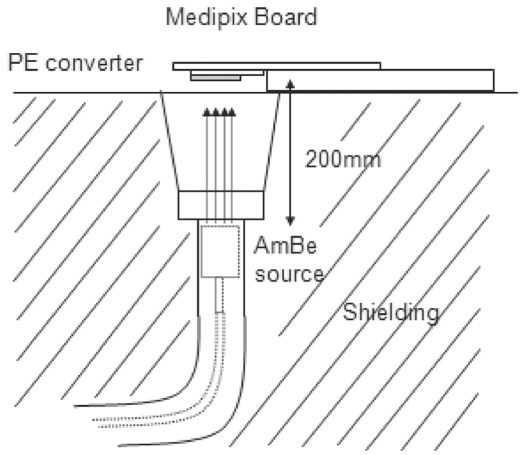

Fig. 5. Irradiation setup on Am-Be neutron source.

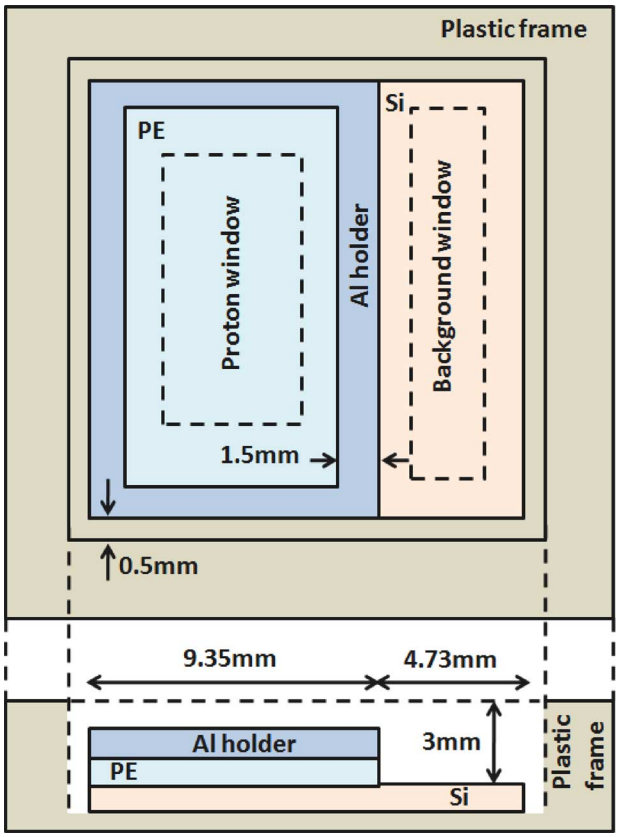

Fig. 4. The Medipix2 with partial PE converter on top of the silicon sensor and uncovered area modeled with GEANT4 (front and side views).

with 65536 pixels) enables the creation of two distinct portions of the sensitive areas to address this issue. Thus the Medipix2 detector is only partially covered with a uniform PE converter layer, noted as SV1 (the proton window), with the reminder left uncovered, noted as SV2 (the background window), and this structure was modeled in the GEANT4 simulation.

The Medipix2 was modeled as a $14.08 \times 14.08 \times 0.3$ mm^3 silicon sensor with 256×256 sensitive volumes, with size $0.055 \times 0.055 \times 0.3$ mm^3. The ASIC chip beneath the silicon sensor was modeled as a silicon slab of size $14.08 \times 14.08 \times 1.5$ mm^3. The PE converter was modeled as a polyethylene slab with thicknesses of 0.1, 0.25, 0.5 and 1 mm, each with a cross section of 9.35×14.08 mm^2. The aluminum holder surrounding the PE converter has been engineered to ensure the converter is rigid and flat, and to minimize air gaps between the PE converter and silicon surface (Fig. 4).

The neutrons are generated as a parallel beam incident normally to the detector. The energy of the neutrons from a simulated D-T source was modeled with a Gaussian distribution, with mean value of 14 MeV and σ of 0.01 MeV and 0.5 MeV. The energy of the neutrons of the Am-Be-source was modeled with the energy spectrum recommended in [27].

QGSP_BIC_HP physics list was used. The threshold of production of secondary particles was fixed equal to 5 μm in range within the sensitive regions SV1 and SV2. In order to reduce the execution times of the simulation without affecting the accuracy of the simulation results, the threshold was set higher outside regions SV1 and SV2.

IV. Experimental Results and Discussion

A. Simplified Setup for GEANT4 Validation

Experiments were carried out on 14 MeV D-T and Am-Be neutron sources at Australia's Commonwealth Scientific and Industrial Research Organisation (CSIRO).

The device was irradiated with 14 MeV neutrons from a D-T generator Thermo A-3062. The distance between the D-T generator and the detector was 55 cm. The emission rate of the D-T generator was 8.6×10^7 n/s into the full solid angle, thus the neutron intensity at the tested detector (area of 1.4×1.4 cm^2) was calculated at 2100 n/s. The D-T generator emission rate was estimated using a $2 \times 2 \times 2$ cm^3 plastic scintillator (EJ 204) attached to a photomultiplier (Photonis XP2020). The detection efficiency of 3.9% of the scintillator for 14 MeV neutrons was approximated by an analytical calculation. The measured neutron flux was in good agreement with the calculated figure.

Fig. 5 shows the irradiation set up on the Am-Be neutron source. The Medipix2 detector was placed on top of the collimator of the Am-Be neutron source container at a distance of 20 cm from the source when in the irradiation position. The PE converter attached to the silicon sensor was faced down normally to the neutron beam. Neutron emission in 4π was 9.3×10^6

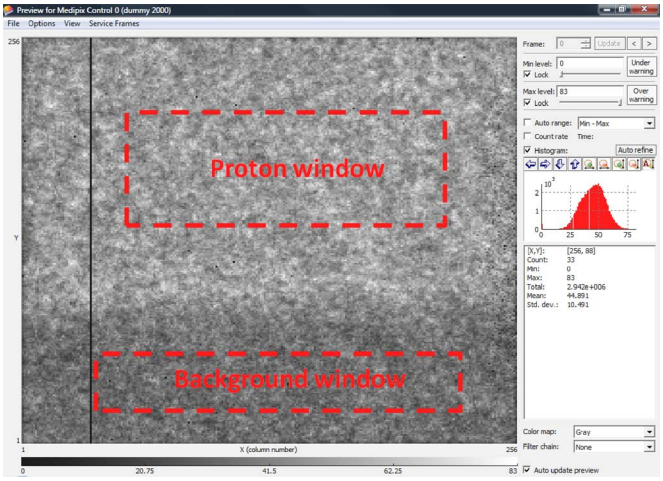

Fig. 6. The events results from fast neutron irradiation. The black line was the dead pixels. The counting windows under PE layer and uncovered area were denoted as proton windows and background windows, respectively.

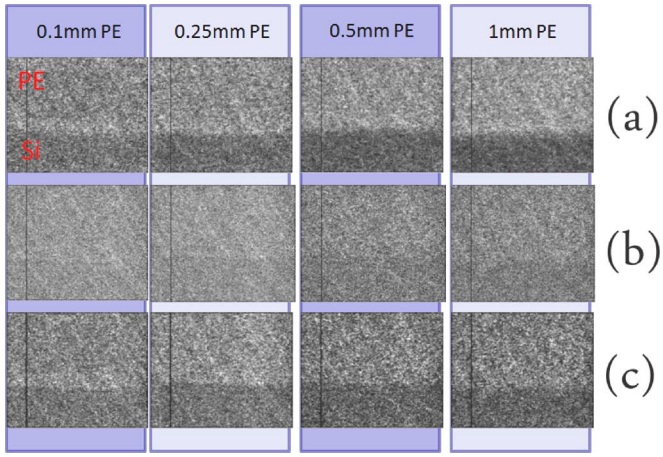

Fig. 7. The total event represented in grey scale modulated image as in Fig. 6. The bright areas show high event counts under PE layer.

n/s calculated based on the activity of the source on the day of the experiment. When not in use the neutron source was kept in boronated paraffin shielding.

The physical construction of the PE converter layer on the Medipix2 detector was as described in Section III.B. The PE converter occupied two-thirds of the active area of the detector, while the other area was uncovered for estimation of the background. A square aluminum frame of $9 \times 14 \times 1$ mm^3 has been used to hold the PE layer attached at the surface of the detector and to minimize the air gap and misalignment between the converter and the silicon substrate (Fig. 4). Four PE thicknesses as modeled in the GEANT4-based study described in Section III.B have been used during the irradiation with the neutron sources. The PE converters were 0.1, 0.25, 0.5 and 1 mm thick.

The detector was placed immediately in front of the neutron source window for both fields with neutrons normally incident to the sensor surface. The experiment was repeated for each thickness of PE using the same Medipix2 detector with the same neutron fluence and geometry of experiment. The data acquisition was based on a USB interface readout by the Pixelman software developed by the Medipix collaboration that provides several analyses and setting tools for use during data acquisition and for data post-processing. During the acquisition the parameters were set to retrieve all data out of the chip from the entire sensitive area.

Fig. 6 shows a screenshot generated by the Pixelman software, representing a grey-scale modulated image of the events in the Medipix2 detector within the SV1 and SV2 areas. A clear difference can be observed between the number of events in the regions of the detector covered by PE (recoil protons and background) and uncovered (background only). Proton and background windows, which were also used in the simulations, are represented in Fig. 6 with a broken red outline. Using these regions inside of SV1 and SV2 inhibits cross-talk, where scattering events from one region are counted in another, therefore improving the accuracy of the neutron response evaluation.

Fig. 7 shows a comparison of the event images for different thicknesses of PE converters irradiated with D-T and Am-Be neutrons. The difference in efficiency of the PE converters of different thicknesses is clearly visible, particularly the increase in efficiency with increased converter thickness observed for exposures with the high energy 14 MeV neutrons (Fig. 7(a)).

Fig. 7(b) and (c) show the event images for the same thicknesses of PE converters but irradiated with neutrons from an Am-Be source, which has a lower average neutron energy ($\sim$ 4.2 MeV) than the D-T source and higher gamma background. This is observed in Fig. 7(b), where due to the larger gamma background the boundary between the SV1 and SV2 regions is not as clear.

In the mixed radiation fields of these experimental setups there were other contributions to the event counts in both counting windows associated with backscattered neutrons, secondary charged particles and a gamma background (Fig. 7). Secondary charged particles, like alphas, contributed the least effect to the counts as they are easily stopped in air. The backscattered neutrons have an almost equal effect on both counting windows as the back of the Medipix2 detector has uniform layers of material.

It is possible to improve the contrast in Fig. 7(b) using features of the Pixelman software that allow filtering of events depending on pixel cluster sizing, which is related to LET of the incident particle. Gamma radiation with low energy photons will deposit energy within a single pixel, whereas higher energy photons will create long tracks due to the higher energy of secondary electrons resulting in energy depositions within more than one pixel [28]. This allows the removal of events corresponding to low energy photons for example which deposit energy in a single pixel only. Fig. 7(c) corresponds to the events of Fig. 7(b) after filtering out events with a cluster size less than 7 pixels. In this case the recoil proton contribution becomes more obvious, which is a further advantage of this dosimeter. Thus the application of cluster size filtration to the experimental data in addition to the background window subtraction method provides improved response of the Medipix2 to neutrons only.

In this study the net proton counts were calculated by subtracting the background counts according to (3) after preliminary cluster size filtration, allowing comparison of the counts produced by recoil protons only for each partial converter. The

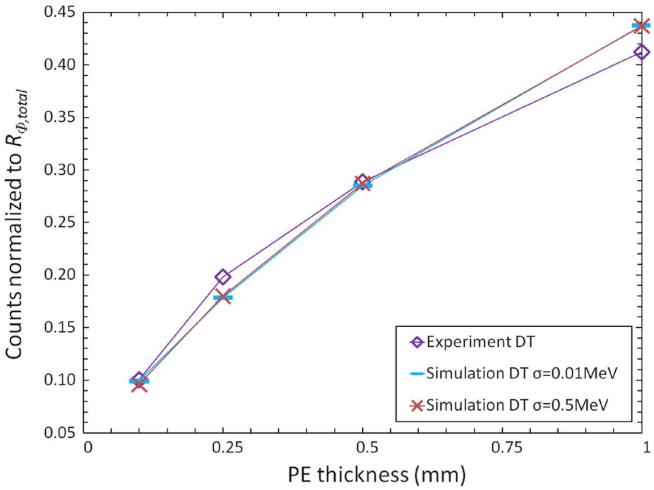

Fig. 8. The comparison of the experimental result of the 14 MeV D-T neutron to that of simulations using Gaussian spectrum of mean 14 MeV and σ of 0.01 and 0.5 MeV.

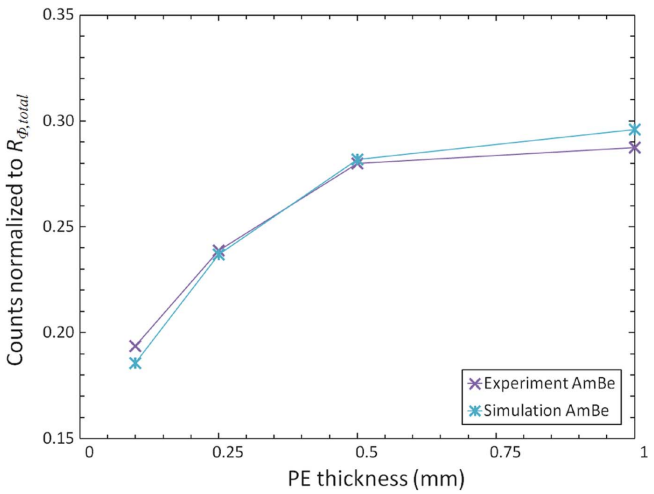

Fig. 9. The comparison of the experimental result of the Am-Be neutron to that of simulation.

response of each converter was normalized to the total number of counts of all converters for the same neutron fluence irradiation as presented in (4). It was used for both the GEANT4 simulations and experiments with D-T and Am-Be sources

$$R_{\Phi,\text{total}} = \sum_{i=1}^{4} R_{\Phi,i}. \tag{4}$$

The data from both neutron field experiments was analyzed further to filter out clusters with a size below seven pixels, which as discussed, removes the background contribution due to the gamma beam that was not included in the GEANT4 simulations.

B. GEANT4 Validation Study Results

Figs. 8 and 9 present the variation of the normalized recoil proton response of the Medipix2 detector with different PE converter thicknesses, showing the direct comparison of the simulation and experiment results for the irradiation with D-T and Am-Be neutron sources, respectively.

For both neutron sources agreement with GEANT4 simulations was within 10%. Error bars for experimental results were too small to be presented resulting from the large number of counts from recoil protons. The detector responses for PE converters with thicknesses of 1 and 0.5 mm in Fig. 9 are not significantly different due to the low average range of the recoil protons produced by neutrons from the Am-Be source. This is in contrast to the behavior of the detector response for 14 MeV neutrons from the D-T source.

The observed agreement between the experimental and simulated results of the dosimeter responses for four PE converters with distinct thicknesses demonstrates the validity of the GEANT4 simulation and of the implemented model of Medipix2 with PE converters. This lends confidence to the optimization procedure, demonstrating that the application of a structured PE converter to a pixilated detector can produce a neutron dosimeter with an energy independent response in the energy range 0.3–15 MeV to within 10%.

A further strength of the application of a pixilated detector such as Medipix2 coupled to structured PE converter for neutron dosimetry is the potential for self-calibration. The optimization process described can be automated being run by an *add-on* software algorithm that automatically adjusts parameters based upon the results of calibration exposures. Several such calibration points would be acquired using a variety of neutron dose equivalent calibration fields, and could be tailored to suit specific radiation fields or neutron energy ranges. Calibrations for individual dosimeters could also allow for variations in commercial production batches. Such a function is not possible with single pad detector dosimeter, but is under development for a pixilated detector such as Medipix2.

Currently astronaut personal dosimetry at the ISS is relying upon on TEPC and some electronic active personal dosimeters. The active personal dosimeters are based on about 350 μm thick, 1×1 cm^2 silicon p-i-n diodes detectors like in LIULIN and DOSTEL [29] and thin silicon p-i-n diodes described in [30], [31] operating in a LET mode followed by conversion of their response to microdosimetry spectra and dose equivalent. These instruments do not providing neutron dose equivalent but rather total dose equivalent as a mixture of neutrons and charged particle fields. Additionally poor representation of micron size spherical or cylindrical type sensitive volumes, with associated variance in chord distributions, produce some distortion in dose equivalent determination. Thick silicon detectors with 350 μm thickness do not allow LET measurements for neutrons with energy below 3–4 MeV because recoil protons with energy below 3 MeV are stoppers in such detectors.

The presented device for neutron dose equivalent measurements for space application has the following potential advantages above currently used dosimeters: 1) measurement of the neutron dose equivalent in mixed neutron-photon-charged particle fields, 2) low neutron energy threshold for fast neutrons (0.25 MeV), and, 3) sophisticated readout techniques and data analysis allowing further development on the same detector for independent measurements of dose equivalent associated with heavy ions. The presented device is not commercially available at this point in time and will require angular dependence characterization as aspect of future research.

V. Conclusion

We have demonstrated the possibility to develop a real time energy independent fast neutron dosimeter for use in mixed radiation fields relevant to space radiation environments.

A pixilated detector, such as Medipix2, is ideally suited to this application due to the high degree of pixilation and parameterization of the response that can be achieved through coupling with a structured variable thickness polyethylene over layer. This approach allows the subtraction of any unwanted radiation background and to therefore estimate the dose due to neutrons only. The high flexibility in response adjustment of such a dosimeter also allows for self-calibration using neutron dose equivalent calibration sources.

Acknowledgment

Authors would like to thanks Medipix Collaboration for providing detectors and support during this project.

References

[1] *NRC, Managing Space Radiation Risk in the New Era of Space Exploration*. Washington, DC: The National Academies Press, 2008.
[2] F. A. Cucinotta *et al.*, "Space radiation cancer risks and uncertainties for Mars missions," *Radiat. Res.*, vol. 156, pp. 682–688, 2001.
[3] F. A. Cucinotta, M. H. Y. Kim, and L. Ren, "Managing lunar and mars mission radiation risks Part I: Cancer risks, uncertainties, and shielding effectiveness," NASA/TP-2005-213164, Houston, TX, 2005.
[4] J. F. Dicello, "HZE cosmic rays in space. Is it possible that they are not the major radiation hazard?," *Radiat. Prot. Dosim.*, vol. 44, no. 1–4, pp. 253–257, 1992.
[5] G. A. Nelson, "Fundamental space radiobiology," *Gravit. Space Biol. Bull.*, vol. 16, no. 2, pp. 29–36, 2003.
[6] ICRU, "The dosimetry of pulsed radiation," *J. ICRU*, vol. Report 34, 1983.
[7] P. D. Bradley, A. B. Rosenfeld, and M. Zaider, "Solid state microdosimetry," *Nucl. Intrum. Methods B*, vol. 184, no. 1–2, pp. 135–157, 2001.
[8] L. Pisacane *et al.*, "Microdosimeter instrument (MIDN) on MidSTAR-I," *SAE Trans. J. Aero.*, vol. 2006-01-2146, 2006.
[9] Wroe *et al.*, "Solid state microdosimetry with heavy ions for space applications," *IEEE Trans. Nucl. Sci*, vol. 54, no. 6, pp. 2264–2271, 2007.
[10] A. L. Ziebell *et al.*, "A cylindrical silicon-on-insulator microdosimeter: Charge collection characteristics," *IEEE Trans. Nucl. Sci*, vol. 55, no. 6, pp. 3414–3420, 2008.
[11] W. H. Lim *et al.*, "Cylindrical silicon-on-insulator microdosimeter: Design, fabrication and TCAD modeling," *IEEE Trans. Nucl. Sci*, vol. 56, no. 2, pp. 424–428, 2009.
[12] L. N. Shyan *et al.*, "Development and fabrication of cylindrical silicon-on-insulator microdosimeter arrays," *IEEE Trans. Nucl. Sci*, vol. 56, no. 3, pp. 1637–1641, 2009.
[13] D. A. Prokopovich, M. I. Reinhard, G. C. Taylor, A. Hands, and A. B. Rosenfeld, "GEANT4 simulation of the CERN-EU high-energy reference field (CERF) facility," *Radiat. Prot. Dosim.*, vol. 141, no. 2, pp. 106–113, 2010.
[14] W. Heinrich, S. Roesler, and H. Schraube, "Physics of cosmic radiation fields," *Radiat. Prot. Dosim.*, vol. 86, no. 4, pp. 253–258, Dec. 1, 1999, 1999.
[15] Mikulec, M. Campbell, E. Heijne, X. Llopart, and L. Tlustos, "X-ray imaging using single photon processing with semiconductor pixel detectors," *Nucl. Instrum. Methods Phys. Res. A: Accel. Spectrom. Detect. Assoc. Equip.*, vol. 511, no. 1–2, pp. 282–286, 2003.
[16] J. Jakubek *et al.*, "Neutron imaging and tomography with Medipix2 and dental micro-roentgenography," *Nucl. Instrum. Methods Phys. Res. A: Accel. Spectrom. Detect. Assoc. Equip.*, vol. 569, no. 2, pp. 205–209, 2006.
[17] M. A. R. Othman *et al.*, "From imaging to dosimetry: GEANT4-based study on the application of Medipix to neutron dosimetry," *Radiat. Meas.*, 2010, doi:10.1016/j.radmeas.2010.06.058, to be published.
[18] Y. Eisen *et al.*, "A small size neutron and gamma dosemeter with a single silicon surface barrier detector," *Radiat. Prot. Dosim.*, vol. 15, no. 1, pp. 15–30, 1986.
[19] F. Shiraishi *et al.*, "A new fast neutron spectrometer made of epitaxial integrated dE-E Si detector," *IEEE Trans. Nucl. Sci*, vol. 32, no. 1, pp. 471–475, 1985.
[20] ICRP, "Conversion coefficients for use in radiological protection," *Ann. ICRP*, vol. 26, no. 3–4, pp. 1–205, 1996.
[21] Medipix2, "The Medipix2 collaboration," 2010, 1/9/2010, [Online]. Available: http://medipix.web.cern.ch/MEDIPIX/Medipix2/indexMPIX2.html
[22] Z. Vykydal *et al.*, "Evaluation of the ATLAS-MPX devices for neutron field spectral composition measurement in the ATLAS experiment," in *Proc. IEEE Nuclear Science Symp. Conf. Record, NSS'08*, pp. 2353–2357.
[23] X. Llopart, "Design and characterization of 64K pixels chips working in single photon processing mode," Department of Information Technology and Media, Mid Sweden Univ.. Sundsvall, Ph.D. dissertation, 2007.
[24] T. Holy *et al.*, "Data acquisition and processing software package for Medipix2," *Nucl. Instrum. Methods Phys. Res. A: Accel. Spectrom. Detect. Assoc. Equip.*, vol. 563, no. 1, pp. 254–258, 2006.
[25] S. Agostinelli *et al.*, "G4—A simulation toolkit," *Nucl. Instrum. Methods Phys. Res. A: Accel. Spectrom. Detect. Assoc. Equip.*, vol. 506, no. 3, pp. 250–303, 2003.
[26] J. Allison *et al.*, "GEANT4 developments and applications," *IEEE Trans. Nucl. Sci*, vol. 53, no. 1, pp. 270–278, 2006.
[27] ISO, "Reference neutron radiations–Part 2: calibration fundamentals of radiation protection devices related to the basic quantities characterizing the radiation filed," 2000, ISO 8529-2.
[28] T. Holy *et al.*, "Pattern recognition of tracks induced by individual quanta of ionizing radiation in Medipix2 silicon detector," *Nucl. Instrum. Methods Phys. Res. A: Accel. Spectrom. Detect. Assoc. Equip.*, vol. 591, no. 1, pp. 287–290, 2008.
[29] G. Reitz *et al.*, "Space radiation measurements on-board ISS—the DOSMAP experiment," *Radiat. Prot. Dosim.*, vol. 116, no. 1–4, pp. 374–379, 2005.
[30] M. Luszik-Bhadra, "Electronic personal neutron dosemeters for high energies: Measurements, new developments and further needs," *Radiat. Prot. Dosim.*, vol. 126, no. 1–4, pp. 487–490, 2007.
[31] M. Luszik-Bhadra, M. Nakhostin, K. Niita, and R. Nolte, "Electronic personal neutron dosemeters for energies up to 100 MeV: Calculations using the PHITS code," *Radiat. Meas.*, vol. 43, no. 2–6, pp. 1044–1048, 2008.